Radio Emission from the Heliopause Triggered by an Interplanetary Shock

D. A. Gurnett, W. S. Kurth, S. C. Allendorf, R. L. Poynter

A strong heliospheric radio emission event has been detected by Voyagers 1 and 2 in the frequency range of 2 to 3 kilohertz. This event started in July 1992 and is believed to have been generated at or near the heliopause by an interplanetary shock that originated during a period of intense solar activity in late May and early June 1991. This shock produced large plasma disturbances and decreases in cosmic ray intensity at Earth, Pioneers 10 and 11, and Voyagers 1 and 2. The average propagation speed estimated from these effects is 600 to 800 kilometers per second. After correction for the expected decrease in the shock speed in the outer heliosphere, the distance to the heliopause is estimated to be between 116 and 177 astronomical units.

The heliopause is the boundary between a hot ($\sim 10^5$ K) ionized gas flowing outward from the sun, called the solar wind (*1*), and the interstellar medium, which is a relatively cool ($\sim 10^4$ K), partially ionized gas between the stars. Because the sun is moving with respect to the nearby interstellar medium, the heliopause is expected to form a teardrop-shaped surface, the nose of which is toward the direction of arrival of the interstellar gas (*2*). The region inside the heliopause is called the heliosphere. Estimates of the distance to the heliopause based on our limited knowledge of the interstellar medium have varied from a few tens to several hundred astronomical units (1 AU = 1.49×10^8 km). For a recent review of the heliosphere and its interaction with the interstellar medium, see Suess (*3*).

Four spacecraft, Pioneers 10 and 11 and Voyagers 1 and 2, are on escape trajectories from the sun to study the outer heliosphere and to penetrate into the interstellar medium. None has yet reached the heliopause or the solar wind terminal shock, which is a standing shock that is expected to form in the supersonic solar wind flow well inside of the heliopause. The radio emission described in this report and its interpretation provide a direct measurement of the distance to the heliopause.

Description of the Event

Frequency-time spectrograms of the radio emission event (Fig. 1) were obtained from the wideband plasma wave system (PWS) on Voyager (*4*), which provides periodic samples of the electric field waveform over a bandwidth of 50 Hz to 10 kHz. Voyager 1 was located at a heliocentric radial distance of $R = 50.8$ AU and a solar ecliptic latitude and longitude of $\beta = 33.6°$ and $\lambda = 245°$ (as of 1 January 1993), and Voyager 2 was located at $R = 39.0$ AU, $\beta = -11.7°$, and $\lambda = 283°$. The spectrograms cover a frequency range from 1 to 4 kHz and a time span of 1 year, from day 120 of 1992 to day 120 of 1993.

Two primary spectral components can be seen in Fig. 1: a main emission band at about 2.0 kHz, and a series of narrowband emissions drifting upward in frequency at a rate of about 3.0 kHz year^{-1}, reaching a peak frequency of about 3.6 kHz. The main band has a sharply defined low-frequency cutoff at 1.8 kHz. Both components must consist of electromagnetic waves because they occur at frequencies well above the local plasma frequency. The plasma fre-

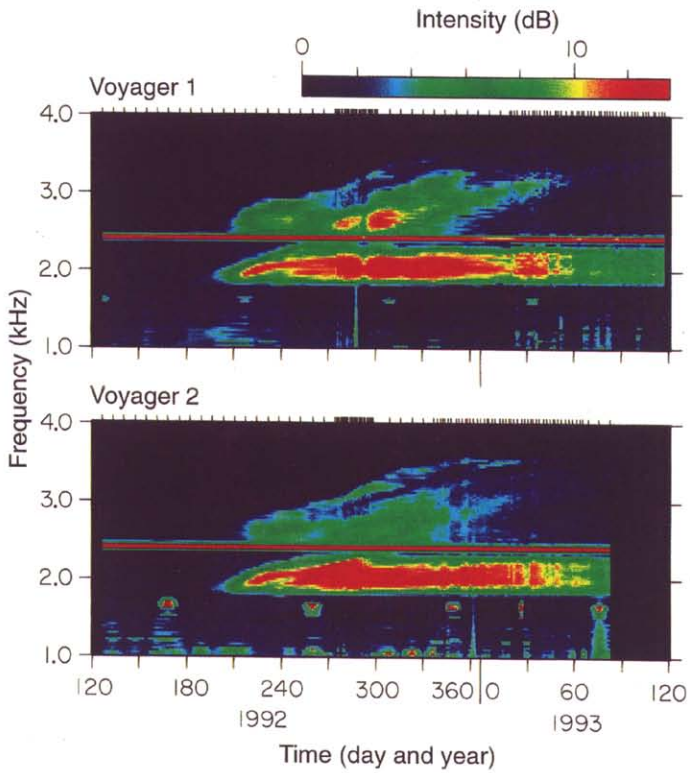

Fig. 1. Frequency-time spectrograms of the 1992–93 heliospheric radio emission event from (top) Voyager 1 and (bottom) Voyager 2. The color indicates the electric field intensity, with red being the most intense and blue being the least intense. Sampling times are indicated by marks at the top of each panel.

D. A. Gurnett, W. S. Kurth, and S. C. Allendorf are in the Department of Physics and Astronomy, University of Iowa, Iowa City, IA 52242. R. L. Poynter is at the Jet Propulsion Laboratory, Pasadena, CA 91109.

quency (f_p = 9000 $\sqrt{N}$ Hz, where N is the electron density in electrons per cubic centimeter) is the low-frequency cutoff of free-space electromagnetic waves and corresponds approximately to the high-frequency limit of locally generated plasma waves. For the time period of interest, the plasma frequency, as determined by the Voyager 2 plasma instrument, ranged from 0.4 to 1.3 kHz, with a mean of around 0.7 kHz (5). The exact starting time of the radio emission is difficult to determine from the wide-band data because the time resolution early in the event is only one spectrum per week (Fig. 1). A more accurate starting time can be obtained from the PWS 16-channel spectrum-analyzer data, which provides one measurement every 16 s. These data show that the radio emission first appeared in the 1.78-kHz channel on day 188 (6 July) of 1992. After the start of the event, the intensity gradually increased over a period of months, reaching a peak in early December 1992. Thereafter, the intensity gradually decreased and was almost down to the receiver-noise level as of July 1993.

A striking characteristic of the overall event is the similarity of the spectrums at the two spacecraft, even though they are separated by 44.6 AU. This similarity suggests that the source is at a considerable distance, greater than 44 AU. From the maximum radiation intensity (1.8×10^{-17} W m^{-2} Hz^{-1}), the radiated power is estimated to be at least 10^{13} W. This radio source is much stronger than any known planetary radio source and is probably the most powerful radio emission in the solar system.

Radio Direction Finding Measurements

Voyager is normally stabilized in a fixed inertial orientation with the high-gain antenna pointed toward Earth. However, once every 3 months, the spacecraft performs a series of rolls around the axis of the high-gain antenna to calibrate the magnetometer. Three such roll maneuvers were performed during the emission event, the first two on days 220 and 311 of 1992 and the third on day 36 of 1993. Because the PWS dipole antenna axis is perpendicular to the roll axis, these maneuvers can be used to perform radio direction finding measurements. The 16-channel spectrum-analyzer data must be used for these measurements because the sample rate of the wide-band spectrum is too low to resolve the roll modulation. Also, because of a data system failure on Voyager 2 shortly after launch, direction finding measurements can only be performed on Voyager 1.

Only two spectrum analyzer channels, 1.78 and 3.11 kHz, are in the proper frequency range to detect the radio emission. No roll-modulation effects were observed in the 1.78-kHz channel. However, a clear roll-modulation signal was observed in the 3.11-kHz channel during all three maneuvers (Fig. 2). The sinusoidal modulation in the electric field intensity at twice the rotation period of the spacecraft is clearly evident. To determine the amplitude and phase of the modulation, we fit a sine function to the data using a least-squares fitting procedure. All three roll maneuvers had similar modulation signatures. The peak-to-peak modulation amplitudes range from about 10 to 20%. These relatively low modulation amplitudes indicate that the source is either relatively large (>60°) or is located well away from the roll axis (~40°), or a combination of these effects. The existence of a significant anisotropy also indicates that the radiation (at 3.11 kHz) is not trapped in a high-Q cavity as suggested by Czechowski and Grzedzielski (6): Multiple reflections in a cavity would be expected to quickly lead to an isotropic electric field distribution.

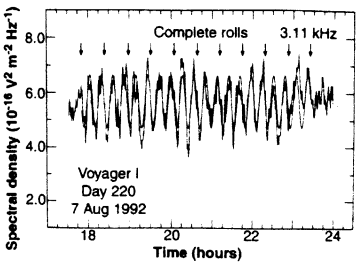

Fig. 2. A plot of the electric field intensity in the 3.11-kHz channel during a 10-turn roll maneuver on day 220, 1992 (11-point sliding average, best fit marked by smooth curve). A clear roll-modulation signal can be seen. The phase of the roll modulation gives the direction to the source.

For a rotating electric dipole, it can be shown that the source must lie in a plane perpendicular to the antenna axis at the time of maximum signal strength, which can be determined from the phase of the roll modulation. If the antenna axis is perpendicular to the roll axis, as it is during these maneuvers, then the plane through the source also contains the roll axis. To visualize possible source locations, it is convenient to construct a diagram looking along the roll axis with all vectors projected onto a plane perpendicular to the roll axis (Fig. 3). In such a diagram, the plane through the source reduces to a line with two possible directions, as shown by the dashed lines with arrows at either end.

The observed source directions tend to cluster around the projected direction of the sun's motion (Fig. 3). The clustering is consistent with a source location near either the nose or the tail of the heliosphere. For the specific geometry involved, the location near the nose or tail turns out to be nearly independent of the distance to the source (<1° variation for distances greater than 100 AU). The variations in the observed source directions were probably related to the fact that the 3.11-kHz channel was responding to the upward-drifting narrowband features (see Fig. 1), which were clearly evolving during the course of the event.

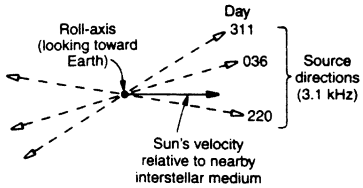

Fig. 3. Source directions at 3.11 kHz determined from roll maneuvers on days 220 and 311, 1992, and on day 36, 1993. The view is from the spacecraft looking along the roll axis (β = −33.7°, λ = 63.7°) toward the Earth. The horizontal (reference) direction has been taken to be the direction of the sun's motion with respect to the nearby interstellar medium (β = 5.0°, λ = 254°), as given by Ajello *et al.* (*24*).

Relation to the Great Forbush Decrease of 1991

Only one previous heliospheric radio emission event has been observed with intensities comparable with those of the 1992–93 event. This event occurred in 1983–84 and was first described by Kurth *et al.* (*7*). Five other extremely weak events have been observed between these two major events (*8*), one in late 1985, one in 1989, and three in 1990–91. Several investigators have searched for unusual effects in the solar wind that might trigger these radio emissions. For example, McNutt (*9*) first suggested that a high-speed solar wind stream could trigger the radio emission when it reached the terminal shock. This idea was explored further by Grzedzielski and Lazarus (*10*), who identified a series of dynamic pressure increases in the solar wind that they believed were responsible for the 1983–84, 1985, and 1989 events. Despite the possible merit of these suggestions, the cause-effect relationship was not convincingly demonstrated, and other sources continued to be considered. For an overview of the situation before the 1992–93 event, see Kurth (*8*).

Because heliospheric radio emission events comparable with the 1992–93 event are extremely rare, one would expect that the solar wind trigger would also be an

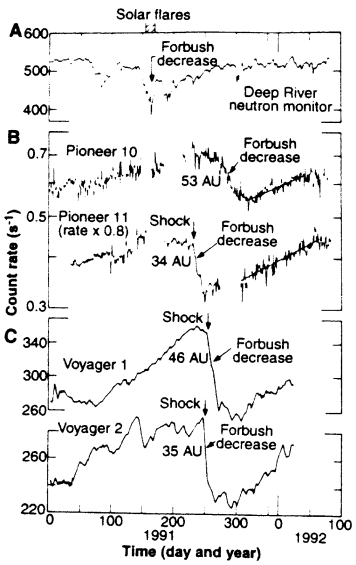

Fig. 4. Cosmic ray counting rates at (**A**) Earth, (**B**) Pioneers 10 and 11 (53 and 34 AU), and (**C**) Voyagers 1 and 2 (46 and 35 AU). The sharp decreases in the cosmic ray counting rates are produced by an outward-propagating interplanetary shock generated by a series of large solar flares in late May and early June 1991. [Adapted from (*14*) and (*15*)].

unusual event. During the period preceding the 1992–93 radio emission event, there is one event, the great Forbush decrease of 1991, that fits this requirement perfectly. For many years it has been known that the sun occasionally ejects an energetic burst of plasma called a coronal mass ejection (*11*). The ejection is often associated with a series of solar flares and produces an interplanetary shock wave that moves outward from the sun at high speed, up to 1000 km s^{-1}. The shock wave is typically followed by a turbulent high-speed stream of plasma. As the shock propagates outward through the heliosphere, the turbulent magnetic fields embedded in the high-speed stream inhibit the entry of cosmic rays, causing a temporary decrease in the cosmic ray intensity. This effect is called a Forbush decrease (*12*).

During the period from 25 May to 15 June 1991, six major solar flares were observed (*13*). This sequence of intense solar activity produced a series of strong interplanetary shocks and one of the largest Forbush decreases ever observed. The main features of this event were first discussed by Van Allen and Fillius (*14*) and Webber and Lockwood (*15*). Shortly after the onset of the period of intense solar activity, a large (~30%) Forbush decrease developed in the data from the Deep River neutron monitor, which records the cosmic ray intensity at the Earth (Fig. 4A). This decrease was the deepest depression in the cosmic ray intensity ever observed by a neutron monitor in over 30 years of observations. Cosmic ray intensities from Pioneer 10 and 11, at 53 and 34 AU (Fig. 4B), and from Voyagers 1 and 2, at 46 and 35 AU (Fig. 4C), were also recorded. As the shocks generated by the solar activity propagated outward from the sun, they are believed to have coalesced into a single shock followed by a region of turbulent high-speed plasma called a merged interaction region (*16*). As the disturbed plasma swept over the Pioneer and Voyager spacecraft, roughly 3 to 4 months after the flare activity, strong decreases occurred in the cosmic ray intensities, first at Pioneer 11, then at Voyagers 2 and 1, and finally at Pioneer 10. The shock itself was also detected, first by the magnetometer on Pioneer 11 (*17*), then by the plasma instrument on Voyager 2 (5), and finally by the plasma wave instrument on Voyager 1 (*14*) (indicated by arrows in Fig. 4). From the timing of the various events, Van Allen and Fillius estimate that the average propagation speed is 820 km s^{-1}. Webber and Lockwood give propagation speeds ranging from 600 to 800 km s^{-1}. The overall propagation time, from the onset of the solar activity on day 145, 1991, to the onset of the radio emission event on day 188, 1992, is 408 days or 1.12 years.

Although the 1992–93 radio emission event and the interplanetary shock associated with the 1991 Forbush decrease are both extraordinary events, one case does not prove a cause-effect relationship. However, upon reexamination of the 1983–84 heliospheric radio emission event, which started on day 242, 1983, a very large (21%) Forbush decrease was found a little over 1 year earlier, on day 195, 1982 (*18*). The time interval between this Forbush event and the onset of the 1983–84 radio emission is 412 days, or 1.13 years, almost exactly the same as the 1992–93 radio emission event. Also, the propagation speeds, 810 and 850 km s^{-1}, given by Van Allen and Randall and by Webber *et al.* (*18*), are almost exactly the same as the speed given by Van Allen and Fillius (*14*) for the 1991 Forbush event. Thus, the two strong heliospheric radio emission events observed by Voyager both appear to have been triggered by interplanetary shocks with large Forbush decreases.

Interpretation of the Radio Emission Spectrum

The frequency-time spectrum of the 1992–93 radio emission event is very complex. To interpret the spectrum, we assume that the radio emission is produced by an interplanetary shock at the plasma frequency (f_p), its harmonic ($2f_p$), or both. The generation of radio emission at f_p and $2f_p$ by an interplanetary shock is well known and is the basic mechanism involved in the generation of type II solar radio bursts (*19*). It is also the only mechanism that has been previously considered as an explanation for the heliospheric radio emissions (*20*).

Three boundaries must be considered as the interplanetary shock propagates outward from the sun: the terminal shock, the heliopause, and the bow shock (Fig. 5). Most previous heliospheric radio emission models have focused on the terminal shock as the source region. However, in this case, the radio emission cannot be generated at the terminal shock or in the region between the terminal shock and the heliopause. The reason is that the electron plasma frequency is too low. Given the observed propagation speed of 600 to 800 km s^{-1} and travel time of ~1.1 years, the terminal shock would have to be located at a distance of 140 to 186 AU. At this great distance, the electron plasma frequency, which varies as $1/R$, would be only about 100 to 150 Hz. Because the electron plasma frequency can only increase by a factor of 2 at a shock and because the highest frequency that can be generated is twice the electron plasma frequency, it would be impossible to generate the observed frequencies.

At the heliopause, the situation is much better. The plasma density at the heliopause is controlled by pressure balance. Because the temperature on the interstellar side of the heliopause is expected to be much colder than on the solar wind side, the electron plasma frequency can increase by a large factor at the heliopause, to a value that is comparable with the plasma frequency in the interstellar medium. From numerical simulations (*21*) and various physical arguments, the plasma-frequency profile in the vicinity of the heliopause is believed to be as shown in Fig. 6. The plasma frequency immediately inside of the bow shock depends on the strength of the bow shock and cannot be more than twice the plasma frequency in the interstellar medium. Remote sensing measurements (*22*) suggest that the electron density in the local interstellar medium is about 0.03 to 0.1 cm^{-3}, which corresponds to a plasma frequency of about 1.6 to 2.8 kHz. These plasma frequencies are in the same general range as the observed radio emission frequencies and are therefore consistent with generation in the vicinity of the heliopause. Just why the radio emission should turn on as the interplanetary shock encounters the heliopause is unknown. Most likely, the onset is related to the much lower temperatures of the interstellar medium, which

would reduce the Landau damping, thereby possibly causing higher radio emission intensities.

Once the interplanetary shock has crossed the heliopause, the emission frequency depends on the plasma frequency encountered by the shock as it propagates through the post-heliopause plasma. Numerical simulations show that there is a pile up of plasma around the nose of the heliosphere (*21*). A cut along the line A-B-C in Fig. 5 would therefore be expected to give a peak in the electron plasma frequency profile, as shown by the curve A-B-C in Fig. 6. A shock propagating through this region would then give an emission frequency that increases with increasing time, as indicated by the curve labeled A-B in the inset to Fig. 6. The rising emission frequency is believed to account for the upward-drifting narrowband emissions evident in Fig. 1. This interpretation also predicts a source near the nose of the heliopause, which is consistent with the direction-finding measurements described earlier. It is not clear whether the radiation is produced at f_p, $2f_p$, or both.

For the segment of the shock front propagating through the flanks of the heliopause, as along line A-B′-C in Fig. 5, the emission frequency should be nearly constant. Radiation from this region is believed to account for the main emission band in Fig. 1, which is nearly constant at a frequency of about 2.0 kHz. In the simplest interpretation, the radiation would not be trapped in the heliospheric cavity. However, the issue of trapping depends sensitively on the details of the plasma frequency profile (which is poorly known) and the exact point where the emission turns on. It is possible that some or all of the radiation generated in the immediate vicinity of the heliopause could be trapped in the heliospheric cavity. The absence of detectable roll modulation in the 1.78-kHz channel does not rule out trapping in this frequency range. We are also not completely certain how to interpret the enhancement at about 2.7 kHz. One possibility is that the main band at 2.0 kHz is caused by emission at the fundamental, f_p, and the enhancement around 2.7 kHz is caused by emission at the harmonic, $2f_p$. An obvious problem with this interpretation is that the ratio of the frequency of the enhancement to the frequency of the main band is only 1.35, which does not indicate a harmonic relation. Similar, though smaller, discrepancies also occur for type II solar radio bursts (*19*). Another possibility is that the 2.0- and 2.7-kHz components are emitted from two regions that have different plasma densities, hence different plasma frequencies. Without more detailed information on the plasma density distribution, it is difficult to distinguish between such interpretations.

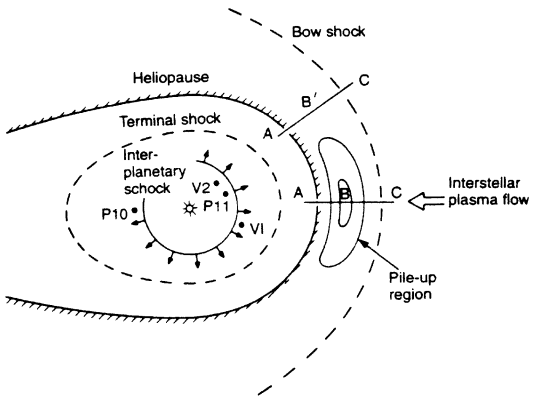

Fig. 5. A sketch of the heliosphere and its anticipated boundaries. The heliopause is the boundary between the solar wind and the interstellar plasma. Because the solar wind is supersonic, a standing shock, called the terminal shock, is expected to form in the solar wind flow well inside of the heliopause. A second standing shock, called the bow shock, is also expected to form in the interstellar plasma flow upstream of the heliosphere. The outward propagating interplanetary shock produced by the solar activity in late May and early June 1991 is indicated by the circle with outward directed arrows. The approximate positions of Pioneers 10 and 11 (P10 and P11) and Voyagers 1 and 2 (V1 and V2) are indicated by the dots. Points A, B, and C correspond with those in Fig. 6.

Finally, we consider the low-frequency cutoff of the spectrum at 1.8 kHz. There are two possible interpretations: first, that it is a propagation cutoff at the plasma frequency, and second, that it is a characteristic emission frequency (either f_p or $2f_p$) in the source. If it is a propagation cutoff, then it most likely corresponds to the plasma frequency in the post-heliopause region well away from the nose of the heliosphere, where the plasma density is comparable with the interstellar value. The electron density in this region would then be about 0.04 cm^{-3}. If the cutoff is a source effect, then the plasma density in the source would be 0.04 cm^{-3} if the emission is at the fundamental, or 0.01 cm^{-1} if it is at the harmonic.

Distance to the Heliopause

The distance to the heliopause can be computed from the propagation speed of the interplanetary shock and the travel time from the sun to the heliopause. The difficulty with this calculation is that the shock almost certainly slows down after passing through the terminal shock. Because the propagation speed in the region beyond the terminal shock is unknown, certain simplifying assumptions must be made. As a simple model, we assume that the shock propagates with a constant speed V_1 inside of the terminal shock and with a slower constant speed V_2 outside of the terminal shock. To take into account the unknown speed V_2, we introduce a speed parameter $\alpha = V_2/V_1$. Because the distance to the terminal shock is also unknown, we also introduce a distance parameter $\delta = R_T/R_H$, which is the ratio of the distance to the terminal shock to the distance to the heliopause. With these two parameters, it can be shown that the distance to the heliopause is given by

$$R_H = V_1 T \frac{\alpha}{1 - (1 - \alpha)\delta} \qquad (1)$$

where T is the total travel time from the sun to the heliopause. For an initial estimate, we use T = 1.1 years and V_1 = 600 to 800 km s^{-1}. These values are consistent with both the 1983–84 and 1992–93 events. For the shock speed parameter α, numerical simulations (*23*) suggest a nominal value of about 0.7, with a range from

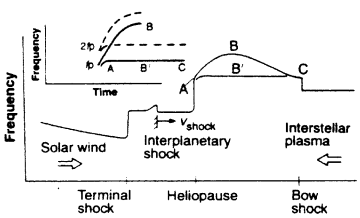

Fig. 6. A representative electron plasma frequency (f_p) profile through the terminal shock, the heliopause, and the bow shock. The peak in the profile along A-B-C (see also Fig. 5) is caused by the "pile up" of plasma near the nose of the heliosphere and is believed to account for the upward-drifting narrowband emissions (Fig. 1). The nearly constant frequency emission at ~2.0 kHz is believed to be produced from the flanks of the heliosphere, along A-B′-C, where the plasma frequency is nearly constant. The 1.8-kHz cutoff would then be indicative of the plasma frequency in this region. (**Inset**) Frequency-time profile.

Table 1. The distance to the heliopause (in astronomical units) as a function of the parameter α (the ratio of the interplanetary shock speed beyond the terminal shock, V_2, to the speed inside the terminal shock, V_1) and the parameter δ (the ratio of the distance to the terminal shock, R_T, to the distance to the heliopause, R_H).

δ (R_T/R_H)	$\alpha = V_2/V_1$		
	0.6	0.7	0.8
	V_1 = 800 km s^{-1}		
0.80	164	172	177
0.75	160	168	175
0.70	155	165	173
	V_1 = 600 km s^{-1}		
0.80	123	129	133
0.75	120	126	131
0.70	116	124	130

0.6 to 0.8. For the distance parameter δ, numerical simulations (*21*) suggest an average value of about 0.75, with a range from about 0.7 to 0.8. The calculations place the distance to the heliopause in the range from about 116 to 177 AU (Table 1). For the nominal value of δ, the distance to the terminal shock is about 87 to 133 AU. With the use of numerical simulations, it should be possible to greatly improve the accuracy of these estimates.

REFERENCES AND NOTES

1. E. N. Parker, *Interplanetary Dynamical Processes* (Interscience, New York, 1963).
2. W. I. Axford, in *Physics of the Outer Heliosphere*, S. Grzedzielski and D. E. Page, Eds. (Pergamon, Oxford, 1990), pp. 7–15.
3. S. T. Suess, *Rev. Geophys.* **28**, 97 (1990).
4. For a description of the Voyager PWS, see F. L. Scarf and D. A. Gurnett, *Space Sci. Rev.* **21**, 289 (1977).
5. J. Belcher, personal communication.
6. A. Czechowski and S. Grzedzielski, *Nature* **344**, 640 (1990).
7. W. S. Kurth, D. A. Gurnett, F. L. Scarf, R. L. Poynter, *ibid.* **312**, 27 (1984).
8. ———, *Geophys. Res. Lett.* **14**, 49 (1987); W. S. Kurth and D. A. Gurnett, *ibid.* **18**, 1801 (1991); W. S. Kurth, *Adv. Space Res.*, in press.
9. R. L. McNutt, *Geophys. Res. Lett.* **15**, 1307 (1988).
10. S. Grzedzielski and A. J. Lazarus, *J. Geophys. Res.* **98**, 5551 (1993).
11. J. D. Gosling *et al.*, *ibid.* **79**, 4581 (1974); S. W. Kahler, *Annu. Rev. Astron. Astrophys.* **30**, 113 (1992); J. D. Gosling, *J. Geophys. Res.*, in press.
12. S. E. Forbush, *Phys. Rev.* **51**, 1108 (1937).
13. *Solar-Geophysical Data*, Prompt Reports, 562-Part 1 (National Oceanic and Atmospheric Administration, Boulder, CO, 1991); *ibid.*, 563-Part 1.
14. J. A. Van Allen and R. W. Fillius, *Geophys. Res. Lett.* **19**, 1423 (1992).
15. W. R. Webber and J. A. Lockwood, *J. Geophys. Res.* **98**, 7821 (1993); see also F. B. McDonald *et al.*, paper presented at the 23rd International Cosmic Ray Conference, Calgary, Canada, 19 to 30 July 1993.
16. L. F. Burlaga *et al.*, *J. Geophys. Res.* **89**, 6579 (1984); L. F. Burlaga, F. B. McDonald, N. F. Ness, A. J. Lazarus, *ibid.* **96**, 3780 (1991).
17. D. Winterhalter, E. J. Smith, L. W. Klein, *Eos* **73**, 237 (1992).
18. J. A. Van Allen and B. A. Randall, *J. Geophys. Res.* **90**, 1399 (1985); W. R. Webber, J. A. Lockwood, J. R. Jokipii, *ibid.* **91**, 4103 (1986).
19. G. B. Nelson and D. B. Melrose, in *Solar Radiophysics*, D. J. McLean and N. R. Lebrum, Eds. (Cambridge Univ. Press, Cambridge, 1985), pp. 333–359.
20. W. M. Macek, I. H. Cairns, W. S. Kurth, D. A. Gurnett, *Geophys. Res. Lett.* **18**, 357 (1991); I. H. Cairns and D. A. Gurnett, *J. Geophys. Res.* **97**, 6235 (1992); I. H. Cairns, W. S. Kurth, D. A. Gurnett, *ibid.*, p. 6245.
21. V. B. Baranov, *Space Sci. Rev.* **52**, 89 (1990); V. B. Baranov and Yu. G. Malama, *J. Geophys. Res.* **98**, 15157 (1993); R. S. Steinolfson, V. J. Pizzo, T. Holzer, in preparation.
22. A. F. Davidsen, *Science* **259**, 327 (1993); R. Lallement, J.-L. Bertaux, J. T. Clark, *ibid.* **260**, 1095 (1993).
23. R. S. Steinolfson, personal communication.
24. J. M. Ajello, A. I. Stewart, G. E. Thomas, A. Garps, *Astrophys. J.* **317**, 964 (1987).

25. We thank the Voyager team at the Jet Propulsion Laboratory (JPL) for their valuable support, especially E. Stone, E. Franzgrote, and S. Linick for scheduling increased wideband coverage during this event, and C. Avis and N. Toy for timely and efficient production of the experiment data records. We also thank R. Lepping for his help in determining the spacecraft attitude during the roll maneuvers. J. A. Van Allen for numerous useful discussions, and L. Granroth, J. Cook-Granroth, and T. Barnett-Fisher for their efforts in processing the data. The research at the University of Iowa was supported by the National Aeronautics and Space Administration through contract 959193 with JPL.